



# Process Development for Phenylethynyl-Terminated PMDA–Type Asymmetric Polyimide Composites

Yixiang Zhang<sup>\*,1</sup>, Atul Jain<sup>1</sup>, Lessa K. Grunenfelder<sup>1</sup>, Masahiko Miyauchi<sup>2</sup>, Steven Nutt<sup>1</sup>

<sup>1</sup>Department of Chemical Engineering and Materials Science, University of Southern California, Los Angeles, CA, USA

<sup>2</sup>Kaneka U.S. Material Research Center, Kaneka Americas Holding, College Station, TX, USA

\* E-mail: zhangyix@usc.edu

**Abstract:** A new type of polyimide, designated TriA X, has been developed for high-temperature composite applications. TriA X is a polymerized monomeric reactant (PMR) type polyimide derived from 1,2,4,5-benzenetetracarboxylic dianhydride, (PMDA), 2-phenyl-4,4'-diamiodiphenyl ether (p-ODA) and phenylethynyl phthalic anhydride (PEPA). The polymer has an asymmetric, non-planar backbone, resulting in an amorphous structure and high toughness. In this work, a TriA X resin (with degree of polymerization  $n=7$  in the imide oligomer) was investigated for processability and performance in carbon fiber composites. Rheological measurements were performed on an oligomer with a low degree of imidization to understand the chemo-rheology of the resin system and determine a suitable B-staging temperature. A composite molding cycle was designed, which yielded fully-consolidated woven carbon fiber laminates. Void contents in panels produced with this molding cycle were  $< 0.1\%$  as measured by image analysis of polished sections, and  $< 0.2\%$  as measured by X-ray micro-computed tomography. Matrix-dominated mechanical properties of composites fabricated with the TriA X polymer exceeded those of PMR-15 composites. These mechanical properties and a measured glass transition temperature of  $367\text{ }^{\circ}\text{C}$  indicate potential for use of this resin system in high-temperature composites.

Please cite the article as: Zhang, Y., Jain, A., Grunenfelder, L. K., Miyauchi, M., & Nutt, S.. “**Process development for phenylethynyl-terminated PMDA-type asymmetric polyimide composites,**” High Performance Polymers (2017), DOI: [10.1177/0954008317720802](https://doi.org/10.1177/0954008317720802)



Key words: Polyimide, asymmetric structure, carbon fiber composites, processing, mechanical properties.

## 1. Introduction

Polyimide composites are often selected for use in high-temperature applications that require both high stiffness and strength and high thermal stability. The high-temperature stability of polyimides stems from unusually strong inter-chain attractive forces.<sup>1</sup> These intermolecular interactions effectively reduce chain mobility and increase chain rigidity, resulting in a high glass transition temperature ( $T_g$ ).

In 1972, NASA Lewis Research Center developed an approach to processing polyimides known as in-situ polymerization of monomeric reactants, or PMR.<sup>2</sup> This technique improved the processability of polyimides compared to prior generation resin systems.<sup>3</sup> One such PMR-type polyimide, PMR-15, is commonly used in high-temperature composite applications. However, cured PMR-15 has a critical drawback - the resin is notoriously brittle (because of a high crosslink density<sup>4</sup>), leading to unavoidable microcracking and degradation during thermal cycling.<sup>5, 6</sup> This shortcoming has historically limited (but not prevented) the use of PMR-15, and since its inception a suitable alternative has been sought.

Over the past few decades, polyimide systems with asymmetric backbones have been synthesized and explored. For example, Hsiao *et al.* prepared a series of polyimides containing asymmetric diaryl ether segments derived from 5-(4-aminophenoxy)-1-naphthylamine, which exhibited enhanced solubility, amorphous structures, and high toughness compared to analogous polyimides based on symmetrical diamines.<sup>7</sup> Likewise, Chern *et al.* incorporated asymmetric di-*tert*-butyl groups into polyimides by imidizing asymmetric diamines and various dianhydrides.<sup>8, 9</sup> The



asymmetric repeat units acted to decrease the intermolecular forces and hence chain packing in the resulting polymers, resulting in excellent solubility, low moisture absorption, and a low dielectric constant.

A thermoset polyimide (UPILEX<sup>TM</sup>-AD) derived from 2,3,3',4'-biphenyltetracarboxylic dianhydride (a-BPDA), 4,4'-oxydiamiline and phenylethynyl phthalic anhydride (PEPA) was developed by Yokota *et al.* and commercialized by Ube Industries Ltd.<sup>10, 11</sup> The distorted/non-planar structure of a-BPDA inhibits intermolecular interactions, preventing dense chain stacking and increasing molecular mobility above the  $T_g$ , thereby improving processability. The asymmetric structure, however, suppresses internal rotation around the biphenyl linkage in the a-biphenyldiimide moiety, and thus the cured polymer exhibits a high  $T_g$ . Composites fabricated with UPILEX<sup>TM</sup>-AD polyimide exhibit greater short-beam strength (SBS) and flexural strength than IM7/PETI-5.<sup>11</sup> Chuang *et al.* developed a polyimide for resin transfer molding (NASA RTM370) that exhibited low viscosity and high  $T_g$ . In the resin, they introduced a-BPDA (as opposed to symmetric 3,3',4,4'-biphenyl dianhydride (s-BPDA)), 3, 4'-oxydianiline, and PEPA, yielding low melt viscosity and greater open-hole compression strength and short-beam shear strength (compared to BMI-5270-1 composites).<sup>12</sup>

Miyauchi *et al.* developed an asymmetric polyimide derived from 1,2,4,5-benzenetetracarboxylic dianhydride (PMDA), 2-phenyl-4,4'-diamiodiphenyl ether (p-ODA) and PEPA.<sup>13-15</sup> This new polyimide system is referred to as "TriA X" for the characteristics of the polymer; Amorphous, Asymmetric, Addition-type and Cross-linked (X). For this work, a TriA X polyimide system (Figure 1) with a 3942 g/mol imide oligomer (n=7) was selected. Previous work on the neat resin system<sup>16, 17</sup> showed that the cured TriA X resin exhibits a high  $T_g$ , thermal stability,



and high toughness and flexibility because of the asymmetric/non-planar unit, p-ODA. Moreover, both the imide oligomer and cured resin have amorphous structures. The properties and characteristics observed in the resin system make TriA X suitable as a potential matrix material for high-temperature structural composites. The manufacturing of such composites, however, poses challenges.

The processing of polyimide composites is difficult not only because of the high melt viscosity of the resin, but also because of the complex chemical reactions that occur during molding. Imidization itself involves the production of alcohol and water as reaction by-products. To obtain void-free parts, these volatile by-products must be removed prior to consolidation and cross-linking. In this work, we present a polymer science-based approach for processing polyimide composites, which is applicable to any PMR-type polyimide resin. To develop this composite molding cycle, chemo-rheology was performed on the neat resin to understand processing characteristics, as well as the effects of B-stage temperature on imidization and cross-linking. Based on the rheological properties of TriA X, a molding cycle for T650-35 8-harness satin (8HS)/TriA X composites was designed and applied to the fabrication of laminates. The laminates produced showed low void contents ( $< 0.1\%$ ) and matrix-dominated mechanical properties superior to those of PMR-15 composites.

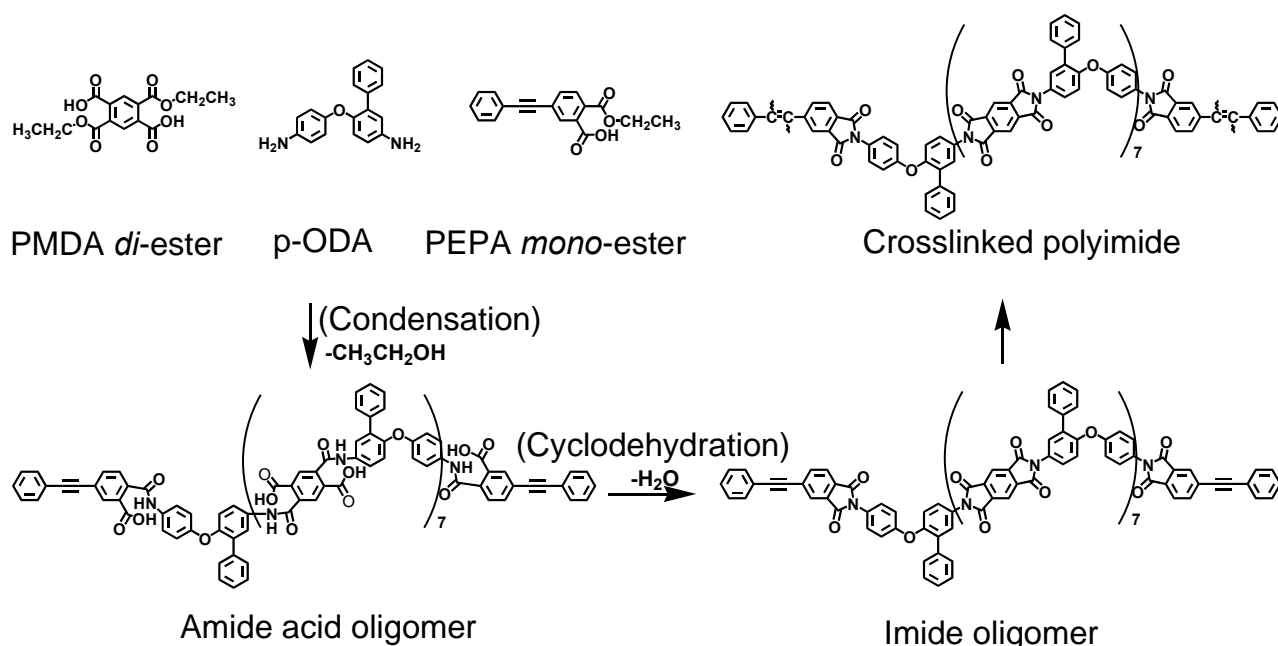


Figure 1. Synthetic scheme of TriA X imide oligomer formulated from PMDA *di*-ester, p-ODA and PEPA *mono*-ester.

## 2. Materials

### 2.1 PMDA *di*-ester/p-ODA/PEPA *mono*-ester Monomers

A powder blend of PMDA *di*-ester/p-ODA/PEPA *mono*-ester (Kaneka, Texas, USA) was utilized in this study. Briefly, PMDA and PEPA were esterified in ethanol, based on the method reported by Houlihan *et al.*<sup>18</sup> After PMDA and PEPA were converted to PMDA *di*-ester and PEPA *mono*-ester, p-ODA was added into the solution with ethanol and heated while stirring, yielding a PMDA *di*-ester/p-ODA/PEPA *mono*-ester solution. The stoichiometric ratios were PMDA *di*-ester: p-ODA: PEPA *mono*-ester= 7: 8: 2, forming an oligomer with a molecular weight of 3945 g·mol<sup>-1</sup> via heat-triggered imidization. Monomer powder was obtained by drying monomer solution at 50 °C under vacuum. The monomer was then stored at room temperature prior to use.

### 2.2 T650-35 8HS/TriA X Prepreg

Please cite the article as: Zhang, Y., Jain, A., Grunenfelder, L. K., Miyauchi, M., & Nutt, S.. “**Process development for phenylethynyl-terminated PMDA-type asymmetric polyimide composites,**” High Performance Polymers (2017), DOI: [10.1177/0954008317720802](https://doi.org/10.1177/0954008317720802)



Prepreg was fabricated using an 80wt% PMDA *di*-ester/p-ODA/PEPA *mono*-ester solution in ethanol, which was combined with de-sized T650-35/8HS/3K carbon fabric (areal weight 368 g/m<sup>2</sup>, Cytec Solvay Group). The prepreg was prepared by calendering the monomer solution on both sides of the fabric. After fabrication, the prepreg was stored in sealed bags at -22 °C prior to use.

### 3. Experiments

#### 3.1 Thermogravimetric Analysis

Thermogravimetric analysis (TGA) of the monomer powder blend was performed under nitrogen purge at a flow rate of 5.00 ml/min (TA Instruments, Q5000). TGA data was obtained to investigate degree of imidization at different B-staging temperatures. Three candidate B-staging temperatures were selected (220 °C, 250 °C and 280 °C) based on the temperature control accuracy of the heated platens used for laminate fabrication. A 4-h degassing step was employed during B-staging to remove volatiles and reaction byproducts from the prepreg stack. 4 hours was selected as a suitable time because of the low gas permeability of the 8HS prepreg.

Monomer powders were dried at 80 °C for 1 h prior to each experiment to remove residual solvent and moisture. The monomers were then imidized for 4 h at 220 °C, 250 °C or 280 °C. Following the 4-h imidization, samples were heated from the imidization temperature to 400 °C at a rate of 5 °C/min. Data acquisition was initiated after the 1-h drying step at 80°C, and continued until completion of the cycle at 400 °C. All monomers were assumed to be fully converted to imide oligomer at 400° C.

The degree of imidization under each thermal condition was determined as the ratio of the percent weight loss at the end of isothermal B-staging ( $W_B$ ) and the percent weight loss at the end of the ramp to 400 °C ( $W_0$ ), as described by Omote *et al.*<sup>19</sup> Mathematically,

Please cite the article as: Zhang, Y., Jain, A., Grunenfelder, L. K., Miyauchi, M., & Nutt, S.. “**Process development for phenylethynyl-terminated PMDA-type asymmetric polyimide composites,**” High Performance Polymers (2017), DOI: **10.1177/0954008317720802**



$$\text{Degree of imidization} = \frac{W_B}{W_0} \times 100\% \quad (1)$$

### 3.2 Rheological Measurements

Rheological measurements were performed using a parallel-plate rheometer (TA Instruments, AR 2000EX). To reduce the influence of bubbling during imidization, the monomer powder blend was heated to 200 °C at a rate of 8.3 °C/min, then quenched to room temperature to obtain an oligomer (Oligomer 0) with a low degree of imidization (85.5%, determined by TGA). Oligomer 0 was ground and pressed at room temperature into 25 mm discs, 0.9-1.1 mm thick, using a hand press (MTI, YLJ-12T).

Pressed oligomer discs were placed on the stationary lower plate of the rheometer, while the upper plate was oscillated at a frequency of 1.0 Hz, and a strain of 0.1 %. The plate gap was adjusted under a normal force control of 1 N to maintain contact with the sample. Complex viscosity ( $|\eta^*|$ ), storage modulus ( $G'$ ), and loss modulus ( $G''$ ) were determined from rheological experiments.

### 3.3 Gel Permeation Chromatography Analysis

The molecular weight change of Oligomer 0 during heating was determined by gel permeation chromatography (GPC) (Shimadzu, Prominence GPC system). Oligomer 0 was heated in a rheometer at 1 °C/min from a starting temperature of 200 °C to a final temperature of 225 °C or 250 °C, to obtain Oligomer 0-1 and Oligomer 0-2, respectively.

The number average molecular weights ( $M_n$ ) of Oligomer 0, Oligomer 0-1 and Oligomer 0-2 were measured using a GPC system with two analytical columns (Phenomenex, Phenogel 5  $\mu\text{m}$ ,  $1 \times 10^4$  Å,  $300 \times 7.8$  mm and Phenogel 5  $\mu\text{m}$ ,  $100$  Å,  $300 \times 7.8$  mm) and a UV detector (Shimadzu,



SPD-20A). The system was calibrated using polystyrene standards. Measurements were performed at 40°C using 1-methyl-2-pyrrolidone as eluent at a flow rate of 1.0 mL/min.

### 3.4 Differential Scanning Calorimetry

Cross-linking in imide oligomers B-staged at different temperatures was investigated using differential scanning calorimetry (DSC) (TA Instruments, Q2000). Tests were performed under nitrogen purge at a flow rate of 50 ml/min. Monomer powder was held for 4 h at 220 °C, 250 °C or 280 °C, after which the resulting oligomers were cooled to 35 °C, then heated to 500 °C at a rate of 10 °C/min. Heat of reaction was determined from the area under the cross-linking reaction peak.

### 3.5 Dynamic Mechanical Analysis

Dynamic mechanical analysis (DMA) was performed to determine the  $T_g$  of cured composite laminates (TA Instruments, Q800). The measurements were carried out in single cantilever mode at a heating rate of 5 °C/min with a fixed frequency of 1 Hz and a strain of 0.3 %. Storage modulus, loss modulus, and  $\tan \delta$  were recorded to determine the  $T_g$  of T650-35 8HS/TriA X composites (described below).

### 3.6 Composite Laminate Fabrication

Laminates (300 × 300 mm) were laid-up at room temperature. The stacking sequences of the laminates produced for this work are shown in Table 1. Fiber volume fraction (FVF) was determined based on the weight and density of the constituent components. For FVF measurements a rectangular coupon was sectioned from each laminate. The dimensions and weight of each coupon were measured by a micrometer and a scale, respectively, and FVF was determined as follows.

$$\text{FVF (vol \%)} = \frac{n \times L \times b \times \rho_f \div \rho_c}{n \times L \times b \times \rho_f \div \rho_c + (M - n \times L \times b \times \rho_f) \div \rho_r} \times 100 \% \quad (2)$$





where:

$n$  = number of prepreg plies;

$L$  = measured specimen length, m;

$b$  = measured specimen width, m;

$\rho_f$  = areal density of T650-35 8HS fabric, 0.368 kg/m<sup>2</sup>;

$\rho_c$  = density of T650-35 carbon fiber, 1.76×10<sup>3</sup> kg/m<sup>3</sup>;

$M$  = measured specimen weight, kg, and,

$\rho_r$  = density of TriA X cured neat resin, 1.29×10<sup>3</sup> kg/m<sup>3</sup>.

Table 1. Molded TriA X/T650-35 8HS laminates.

Laminate No.	Lay-up sequence	Thickness (mm)	FVF (vol %)
1	[0/+45/-45/90] <sub>s</sub>	3.120	55.1
2	[0/90/-45/+45/0/90] <sub>s</sub>	4.607	55.6
3	[0/+45/-45/90] <sub>s</sub>	3.097	55.1
4	[0/+45/-45/90] <sub>2s</sub>	6.237	56.6

After layup, each prepreg stack was dried at 50 °C for 24 h in a convection oven, then vacuum bagged using a polyimide film. Bagged laminates were cured in a hot press. Details of the cure cycle (oven and hot press) are described in section 4.3.

### 3.7 Porosity Measurement

Image analysis (IA) and X-ray micro-computed tomography (micro-CT) were employed to investigate the porosity of manufactured laminates. Two samples, 20-25 mm long, were cut from the center of each laminate for IA. The samples were mounted in potting resin, polished, and imaged



using a digital microscope (Keyence, VHX-600). Void content was determined by the area fraction of voids (visible in the cross section) using image analysis software (Adobe Photoshop and ImageJ).

For validation of microscopy results, high-resolution X-ray tomography was performed on the thickest laminate, which can be expected to have the highest void content. A section ( $20 \times 20 \times 6$  mm) was removed from the center of a 16-ply sample with a stacking sequence of  $[0/+45/-45/90]_{2s}$  and scanned (Nikon, XT H 225ST). Mo- $K_{\alpha}$  incident radiation ( $\lambda=0.71 \text{ \AA}$ ) was used with 60 kV/220  $\mu\text{A}$  voltage/intensity settings to achieve a resolution of  $14.596 \mu\text{m}$  per pixel. The x-ray attenuation of fiber and matrix is relatively high, while the signal attenuation of voids (air) is low. Voids were recognized based on attenuation differential, and the volume fraction of voids was determined using an image analysis utility (Visual Studio Max).

### 3.8 Mechanical tests

The tensile, flexural, and short-beam shear (SBS) properties of T650-35 8HS/TriA X composites were measured at room temperature in accordance with ASTM D3039<sup>20</sup>, ASTM D7264 (four-point bending procedure)<sup>21</sup> and ASTM D2344<sup>22</sup> standards, respectively. This series of tests yielded stiffness and strength properties of the composite when subjected to tensile, bending and shear loads, thus providing holistic information about key mechanical attributes. While tensile and flexural properties of composites depend on fiber properties, SBS properties depend primarily on the properties of the matrix material.

Tensile tests were conducted using a high-capacity load frame (Instron, 5585H) at a displacement rate of 2 mm/min. The flexural and SBS tests were performed on a smaller load frame (Instron, 5567) at a crosshead displacement rate of 1.0 mm/min. Displacement was measured using an extensometer



(Instron, 2630-109) and a deflectometer (Instron, 2601-093) for tensile tests and bending tests, respectively.

## 4. Results and Discussion

### 4.1 Processability

#### 4.1.1 Chemo-rheological Properties

During the processing of PMR-type polyimides, monomers first condense to form amid acid oligomers, then cyclodehydrate, closing imide rings and forming imide oligomers. Cyclodehydration occurs at relatively low temperatures (200-300 °C), releasing volatile by-products. Following this imidization reaction, the oligomer softens and then cross-links at high temperatures (300-400 °C), forming the final thermoset polyimide. Each step of the cure involves viscosity changes, making viscosity measurements critical to determination of suitable process parameters. Chemo-rheology of the resin system was studied to identify relationships between chemical reactions, viscosity changes, and temperature.

The dynamic rheological behavior of an oligomer (Oligomer 0) with a low degree of imidization (85.5%) was evaluated at a heating rate of 1 °C/min. To illustrate the viscosity changes, dynamic rheological data from 200 °C to 400 °C is shown in Figure 2a. Complex viscosity ( $|\eta^*|$ ), storage modulus ( $G'$ ), and loss modulus ( $G''$ ) are presented. A viscoelastic fluid will exhibit solid-like or liquid-like behavior under different thermal conditions. The storage modulus represents the elastic or solid-like component, while the loss modulus represents the viscous or liquid-like component. When  $G' > G''$ , the material exhibits viscoelastic solid-like behavior. Conversely, when  $G' < G''$ , the material behaves as a viscoelastic liquid.

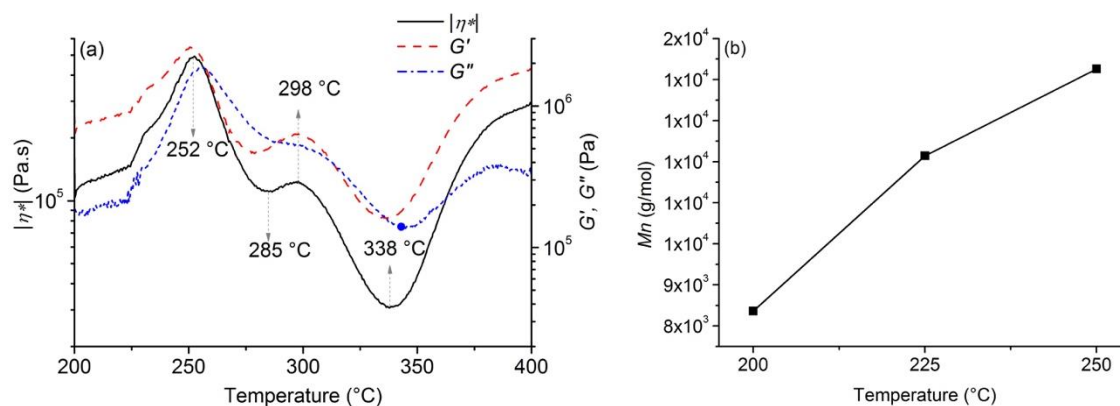


Figure 2. (a) Dynamic  $|\eta^*|$ , (black solid),  $G'$  (red dash) and  $G''$  (blue short dash) profiles for Oligomer 0 at a ramp rate of 1 °C/min, and (b)  $M_n$  change of Oligomer 0 upon heating during rheological measurement.

During rheological measurements of TriA X, multiple transitions were observed. Below 252 °C,  $|\eta^*|$  was high, and the resin was a solid ( $G' > G''$ ). The increase in modulus observed as the temperature increased to 252 °C is a result of both the increase in molecular weight occurring during imidization (Figure 2b), and a gradual and continuous softening of the oligomer, which can effectively enhance the interfacial connection between the specimen and the rheometer plates.<sup>23</sup> When a resin behaves as a rigid solid, the parallel plates in the rheometer can slip past the specimen, resulting in a low apparent viscosity. When the oligomer begins to soften, adhesion to the plates increases, increasing frictional contact. This behavior was observed in the TriA X system. At 252 °C, the viscosity began to drop, reaching a local minimum at 285 °C. In this temperature range, the resin exhibited liquid-like behavior ( $G' < G''$ ), indicating that the oligomer began to soften at 252 °C. The minimum in the  $|\eta^*|$  curve at 285 °C is attributed to residual imidization, as discussed below.

TGA and rheological measurements were performed on Oligomer 0 to confirm that residual imidization was responsible for the minimum  $|\eta^*|$  observed at 285 °C (Figure 2a). A dynamic TGA measurement of Oligomer 0 at 1 °C/min revealed weight loss between 161 °C and 300 °C (Figure Please cite the article as: Zhang, Y., Jain, A., Grunenfelder, L. K., Miyauchi, M., & Nutt, S.. “**Process development for phenylethynyl-terminated PMDA-type asymmetric polyimide composites,**” High Performance Polymers (2017), DOI: [10.1177/0954008317720802](https://doi.org/10.1177/0954008317720802)



3a), consistent with off-gassing. This off-gassing behavior indicates that imidization was taking place in this temperature range. If the drop in viscosity was due to residual imidization, as hypothesized, the minimum  $|\eta^*|$  observed at 285 °C in the initial rheological data would not appear in a secondary heating of a sample. Indeed, we observed that when a single resin sample was subjected to a second temperature ramp from 200 °C to 400 °C (after initial heating to 310 °C) the local viscosity minimum at 285 °C was no longer observed (Figure 3b). The absence of this feature during the second heating cycle confirmed that the minimum  $|\eta^*|$  at 285 °C was the result of a chemical reaction.

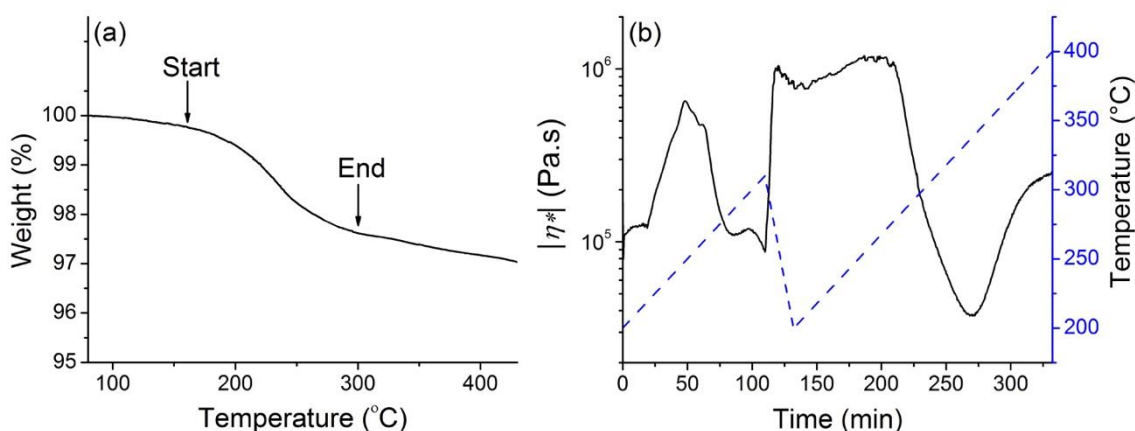


Figure 3. (a) Weight loss (TGA) and (b) complex viscosity of Oligomer 0.

Two possible reactions can occur during residual imidization. The first is a condensation reaction between ester groups and amino groups, generating ethanol. While the extent of this reaction is small, the resulting change in the molecular weight of the oligomer is significant, resulting in an expected increase in complex viscosity. The second possibility is a cyclodehydration reaction, in which the amide acid oligomer is converted to the imide oligomer, generating water molecules. The difference in the viscosities of the two oligomers is assumed to cause the change in the complex viscosity profile at 285 °C.

Please cite the article as: Zhang, Y., Jain, A., Grunenfelder, L. K., Miyauchi, M., & Nutt, S.. **“Process development for phenylethynyl-terminated PMDA-type asymmetric polyimide composites,”** High Performance Polymers (2017), DOI: [10.1177/0954008317720802](https://doi.org/10.1177/0954008317720802)



Between 289 °C and 314 °C, the dynamic rheology measurements of Oligomer 0 revealed that  $G'$  exceeded  $G''$ , indicating that the imide oligomer solidified in this temperature range (Figure 2). Above 298 °C, imidization was nearly complete, although the increasing temperature resulted in re-softening of the resin. Thus,  $G'$  once again dropped below  $G''$ , and the resin behaved as a viscoelastic liquid. The minimum in the complex viscosity curve ( $|\eta^*|_{\min}=3.1\times10^4$  Pa.s) was observed at 338 °C. This was attributed to the cross-linking reaction of PEPA. Above 338 °C, the viscosity increased sharply, as the imide oligomer cross-linked into a stiff, cured thermoset. Note that the two modulus curves crossed at 336 °C. This crossover point is generally defined as the gel point of the resin, providing an estimate of the temperature and time at which the resin formed an infinite network of cross-links.

Overall, the resin began to soften at 252 °C, and as temperature continuously increased, residual imidization was triggered and dominated the viscosity change at 285 °C, resulting in a slight increase in viscosity between 285 °C and 298 °C. Above 298 °C, residual imidization was nearly complete, and resin softening dominated again, leading to a decrease in viscosity. The primary minimum viscosity ( $|\eta^*|_{\min}=3.1\times10^4$  Pa.s) was observed at 338 °C, above which the cross-linking reaction markedly increased the resin viscosity.

#### 4.1.2. Effect of B-staging Temperature

The purpose of a B-staging procedure in polyimide processing is to maximize the degree of imidization of the oligomer prior to the final crosslinking reaction. In PMR resin systems imidization and cross-linking either occur independently, or the two reactions partially overlap in an intermediate temperature range. The first scenario (Figure 4a) is generally preferred for the processing of composite materials, as consolidation pressure can simply be applied after the resin is fully imidized.



In the second type of system (Figure 4b), of which TriA X is one, imidization and crosslinking cannot be separated completely. In this case, low B-staging temperatures generate oligomers with a low degree of imidization and high volatile content which is difficult to remove in subsequent steps of oligomer softening and laminate consolidation. B-staging at higher temperatures, however, can trigger cross-linking, raising the viscosity of the resin system, and thus increasing the difficulty of consolidating laminates. Therefore, the B-staging temperature must be tailored for this type of PMR resin system to achieve an acceptable trade-off between imidization and crosslinking.

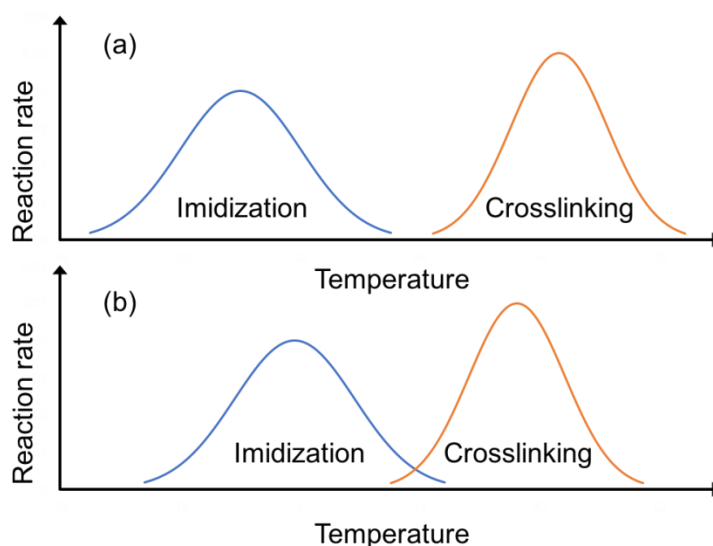


Figure 4. Imidization and crosslinking relations in PMR polyimides: (a) isolation and (b) overlap.

Rheology, DSC, and TGA were used to determine the effects of three potential B-staging temperatures (220 °C, 250 °C and 280 °C) on resin viscosity, crosslinking, and imidization. Rheological measurements were performed on Oligomer 0 (low degree of imidization at 85.5%) to reduce the effects of volatile-induced bubbling during initial imidization on viscosity results. Three rheological cycles were investigated, as summarized in Table 2. For each cycle, Oligomer 0 was initially heated from room temperature to the B-staging temperature and equilibrated for 10 min



prior to the start of data collection. Following this equilibration, a 4 h isothermal hold was performed at each B-staging temperature. At the end of the isothermal hold the resin was heated to 400 °C at a rate of 1 °C/min. Viscosity data for all three cycles are presented in Figure 5. The effect of B-staging temperature on viscosity changes in each cycle is discussed below.

**Cycle 1:** Changes in the  $|\eta^*|$  profile were observed only in the initial 30 min of the isothermal hold, a result attributed to rapid imidization. Following the initial increase,  $|\eta^*|$  was approximately constant during the isothermal hold, stabilizing at  $4 \times 10^5$  Pa·s, indicating that no further reaction (i.e., cross-linking) occurred. The oligomer B-staged at 220 °C exhibited a  $T_g$  of 240 °C (determined by DSC). During the final temperature ramp to 400 °C,  $|\eta^*|$  initially increased (up to 251 °C) because the oligomer softened, which increased the interfacial adhesion between the resin and the parallel plates. With continued temperature increase, the oligomer continued to soften, displaying a local viscosity minimum at 281 °C, characteristic of residual imidization. The minimum  $|\eta^*|$  ( $2.26 \times 10^4$  Pa·s) in Cycle 1 occurred at 340 °C.

**Cycle 2:** In Cycle 2,  $|\eta^*|$  was again approximately constant ( $1.3 \sim 1.4 \times 10^6$  Pa·s) during the isothermal hold, although it was greater than observed with the lower temperature cycle. The  $T_g$  of the oligomer (251 °C, determined by DSC) was similar to the B-staging temperature (250 °C). As with Cycle 1, a constant  $|\eta^*|$  during the isothermal hold indicated that no cross-linking occurred after the initial imidization. As temperature increased after the isothermal hold, the resin softened and exhibited signs of residual imidization in the form of a local viscosity minimum at 290 °C. The minimum  $|\eta^*|$  ( $4.06 \times 10^4$  Pa·s) in the cycle occurred at 338 °C.

**Cycle 3:** The viscosity behavior for Cycle 3 differed markedly from that observed in lower temperature B-staging cycles. The initial  $|\eta^*|$  ( $1.3 \times 10^5$  Pa·s) during the isothermal hold was less





than the values for Cycle 1 and Cycle 2, because the dwell temperature was greater than the  $T_g$  of the oligomer (260 °C, determined by DSC), and thus the resin was soft at the start of the dwell. However, during the isothermal hold,  $|\eta^*|$  increased continuously, indicating the contribution of a cross-linking reaction. No residual imidization was observed during the final temperature ramp in Cycle 3. The minimum  $|\eta^*|$  ( $5.00 \times 10^4$  Pa · s), occurred at 326 °C.

Table 2. Cycles for rheological measurements with ramps from isothermal holds to 400 °C at 1 °C/min.

Cycle name	B-staging	$ \eta^* _{\min}$ (Pa · s)	$T_{ \eta^* _{\min}}$ (°C)	$T_g$ of oligomer (°C)
Cycle 1	220 °C/4 h	$2.26 \times 10^4$	340	240
Cycle 2	250 °C/4 h	$4.06 \times 10^4$	338	251
Cycle 3	280 °C/4 h	$5.00 \times 10^4$	326	260

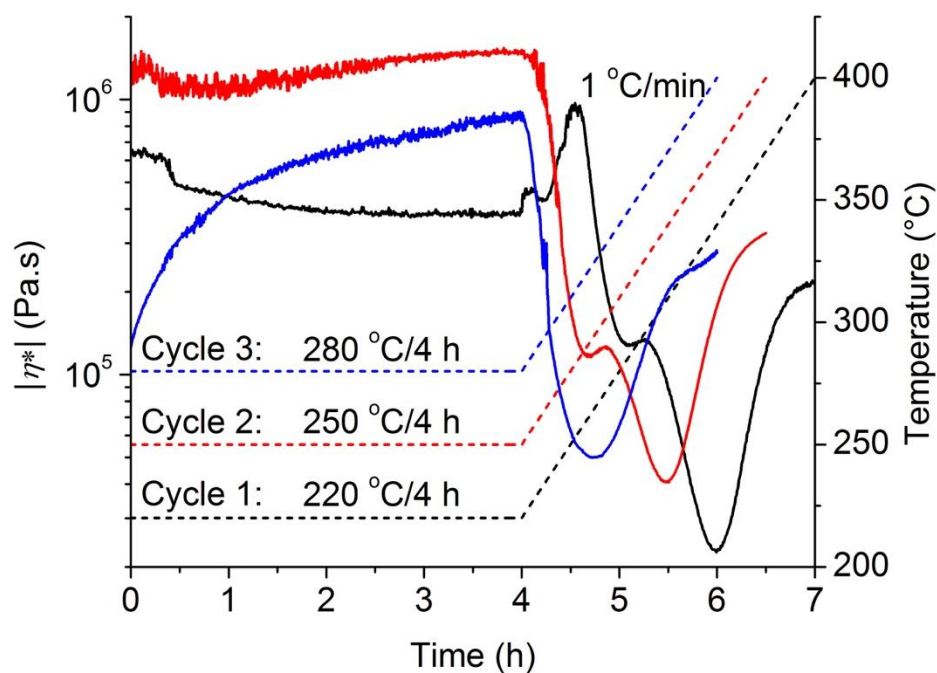


Figure 5.  $|\eta^*|$  profiles (solid lines) and temperature profiles (dash lines) of the B-staged TriA X resins in Cycle 1 (black), Cycle 2 (red) and Cycle 3 (blue).

The higher value of minimum  $|\eta^*|$  in Cycle 3 relative to Cycles 1 and 2 was attributed to more extensive cross-linking. While the reaction rate was relatively slow at 280 °C, the long heating time generated a non-negligible degree of cross-linking, resulting in an increase in minimum  $|\eta^*|$ . The crosslinking reaction at 280 °C was also evident in DSC results (Figure 6 – blue bars). The oligomer B-staged at 280 °C exhibited a lower heat of reaction, while the oligomers B-staged at 220 °C and 250 °C displayed comparable heats of reaction.

Heat of reaction was measured via DSC scans of the oligomers from 35 °C to 500 °C. Any crosslinking during B-staging causes a reduction in the heat of reaction at the cure temperature, because some end caps react during B-staging. Therefore, the heat of reaction for oligomers B-staged at 220 °C (37.5 J/g), 250 °C (37.2 J/g) and 280 °C (24.3 J/g) for 4 h revealed a cross-linking reaction at 280 °C, while no cross-linking was observed at 220 °C or 250 °C.



Finally, TGA was performed on oligomers following each B-staging procedure (with Oligomer 1 corresponding to Cycle 1, etc.) to determine the degree of imidization for each isothermal condition. As expected, a lower B-staging temperature resulted in a lower degree of imidization (Figure 6 – red bars). For the B-staging conditions examined here, Oligomers 2 and 3 exhibited similar degrees of imidization (97.2 and 98.5%, respectively), while Oligomer 1 showed a slightly lower degree of imidization (94.4 %). As discussed previously, a low degree of imidization is not desirable because, during subsequent heating steps, partially imidized oligomers generate volatiles which are difficult to remove and can lead to defects in finished parts.

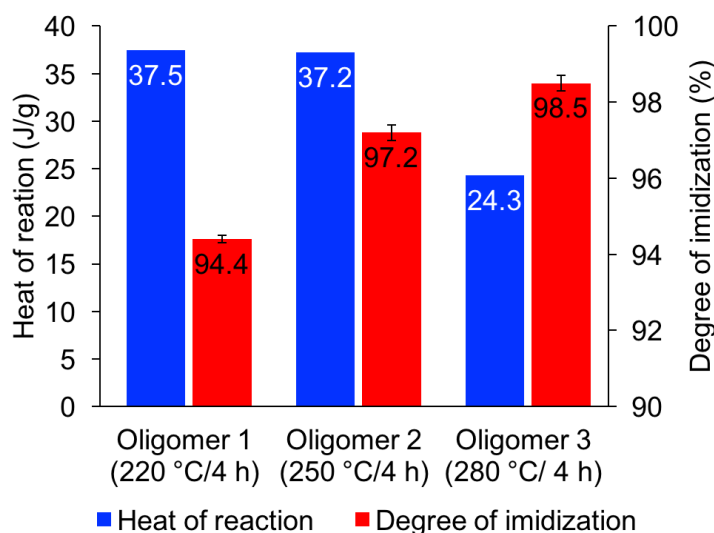


Figure 6. Heat of reaction and degree of imidization of the B-staged TriA X resins.

The goal of B-staging is to achieve a high degree of imidization while avoiding the onset of cross-linking. For the TriA X system, B-staging at 280 °C produced a high degree of imidization but also initiated cross-linking, leading to a high melt viscosity and thereby reducing processability. No cross-linking was observed in samples B-staged at 220 °C or at 250 °C, but the degree of imidization was increased to 97.2 % at the higher temperature. Based on the principle of “*maximum imidization*



*without cross-linking*”, a suitable B-staging temperature of 250 °C was selected (among the three candidate temperatures) for the fabrication of composite laminates.

## 4.2 Composite Fabrication

Relying on the thermochemical data, a molding cycle was developed for unstaged T650-35 8HS/TriA X prepreg. This molding cycle consisted of two parts - the first carried out in an air-circulating oven, and the second in a heated press (Figure 7). In the oven cycle, the prepreg stack was heated to 50 °C for 24 h to remove solvent (ethanol). At this stage in the process, the viscosity of the monomer solution was low (<10 Pa.s at 50 °C~70 °C), and thus drying in a vacuum bag assembly would cause unacceptable resin bleed. For this reason, no vacuum was applied during the drying step. Additionally, the 8HS fabric used in the prepreg had relatively low gas permeability, rendering solvent removal difficult and slow. When the temperature is close to or above the boiling point of ethanol, the evaporation rate is rapid, and the prepreg plies exhibit “ballooning”, which can lead to ply misalignment and wrinkling. To avoid these issues, drying was performed slowly and at a moderate temperature (50 °C).

After drying, the prepreg stack was bagged using a polyimide film (for thermal stability) and cured in a heated press. An envelope bag assembly was used, with bagging film on both sides of the laminate stack sealed along the perimeter with vacuum sealant tape. This approach allowed positioning of the vacuum port and sealant tape outside the hot zone of the press platens during consolidation and cure. A schematic of the bagging sequence (Figure 8) shows that the lay-up is symmetric, with the prepreg as the mirror plane.



Process parameters such as vacuum level/time of application, B-staging temperature and duration, heating rates, and consolidation temperature and pressure, were selected to obtain high quality laminates. Key steps in the hot-press cycle consisted of:

a. Initial temperature ramp from room temperature to 250 °C at 7.5 °C/min. The rate (the maximum heating rate of the hot press) was constant during the ramp. During the ramp, the monomer mixture began to imidize and volatiles were generated. Three vacuum pressure conditions were evaluated for this step, and a final selection was made based on experimental observations.

i. Full vacuum: The complex viscosity of the monomer mixture showed a minimum value of 2.5 Pa · s at 130 °C. At this temperature, the monomer mixture melted. The pressure difference between full vacuum and atmosphere yielded extensive resin bleed.

ii. No vacuum: During imidization, water and alcohol by-products formed, but in the absence of applied vacuum, volatiles could not escape the bag assembly. Elevated pressure within the bag caused the fabric to balloon, resulting in uneven laminates.

iii. Partial vacuum (10% of -101 kPa): Under conditions of reduced vacuum, reaction by-products were able to flow out of the prepreg and exit the vacuum bag. With a low degree of vacuum, neither bleeding nor ballooning occurred.

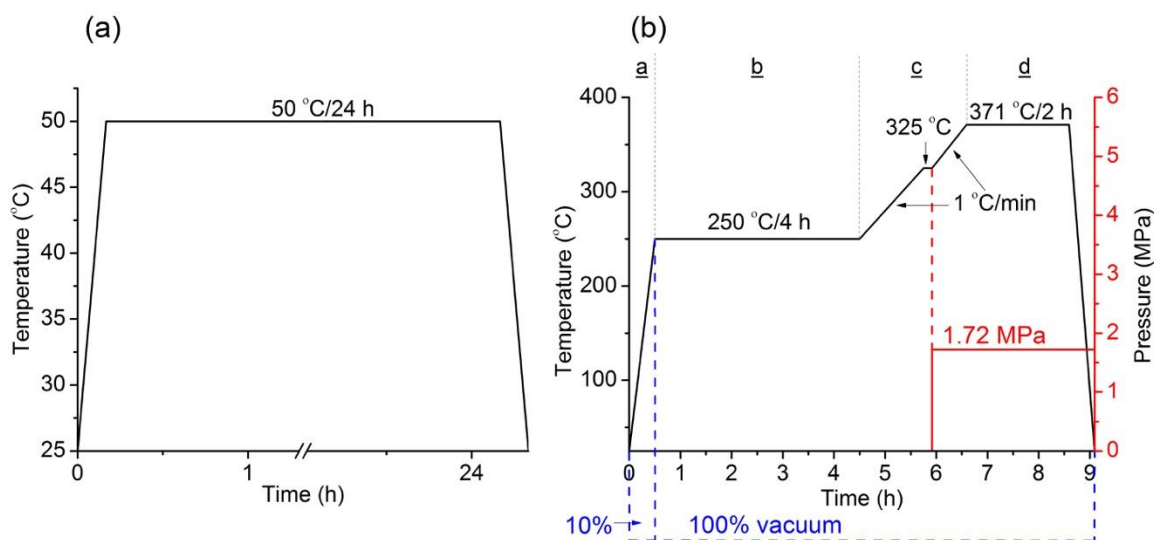
Based on these observations, partial vacuum was selected for the first ramp from room temperature to 250 °C.

b. B-staging at 250 °C. As discussed previously, B-staging was carried out to increase the degree of imidization. During B-staging, full vacuum was applied to remove reaction by-products. Because of the low gas permeability of the 8HS fabric, the prepreg was degassed for 4 h to ensure that all the volatiles were evacuated.



c. Consolidation at 325 °C. As temperature was increased following B-staging, residual imidization occurred with a corresponding release of by-products. A slow ramp rate (1 °C/min) was therefore applied to facilitate evacuation of volatiles. After a 10-min isothermal hold at 325 °C, pressure was applied to consolidate the laminate (1.72 MPa). Prior to applying pressure, a two-minute bump sequence was performed to evacuate volatiles. To obtain void-free parts, imidization by-products must be removed before the application of pressure<sup>23</sup>. If by-products remain in the laminate following consolidation, the only path for volatile escape is through diffusion (which is prohibitively slow), and volatiles trapped in the laminate will result in voids. As residual imidization is completed at 300 °C, a consolidation temperature of 325°C was chosen to ensure that no volatiles were trapped. Given the limits of the heating control of the press, a ten-minute hold at this consolidation temperature was introduced into the molding cycle to allow time for thermal equilibration prior to application of pressure.

d. Cure at 371°C. A final isothermal hold was performed to facilitate crosslinking, yielding a laminate with a  $T_g$  of 349 °C (onset of storage modulus drop), 358 °C (peak of loss modulus) or 367 °C (peak of  $\tan \delta$ ).



Please cite the article as: Zhang, Y., Jain, A., Grunenfelder, L. K., Miyauchi, M., & Nutt, S.. “**Process development for phenylethynyl-terminated PMDA-type asymmetric polyimide composites,**” High Performance Polymers (2017), DOI: [10.1177/0954008317720802](https://doi.org/10.1177/0954008317720802)



Figure 7. Molding cycle for TriA X/T650-35 8HS: (a) Oven cycle and (b) hot press cycle.

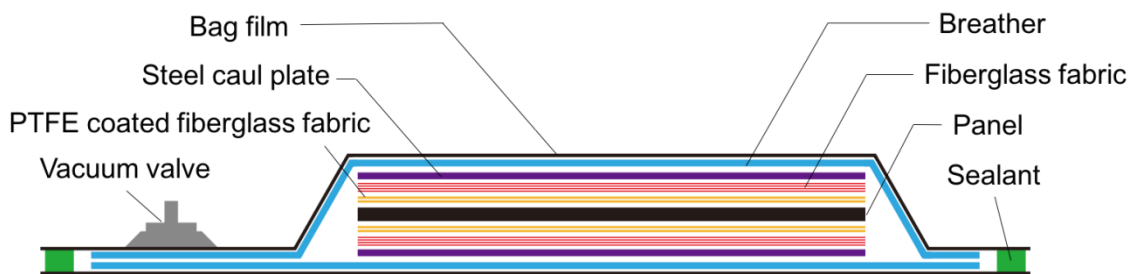


Figure 8. Bagging scheme for TriA X/T650-35 8HS.

The molding procedure described above was used to produce void-free laminates with T650-35 8HS/TriA X. Figure 9 shows the cross section of a 16-ply laminate, c. 6 mm thick. The void content of the laminate, determined by IA, was 0.04 %, and the 3-dimensional void content determined by micro-CT was 0.18 %.



Figure 9. TriA X/T650-35 8HS laminate with a lay-up of  $[0/+45/-45/90]_{2s}$ .

### 4.3 Composite Properties

Tensile, flexural, and SBS tests were performed on void-free laminates at room temperature. Specimen stacking sequences, dimensions, fiber volume fractions, and void contents are shown in Table 3. Prior to mechanical testing, all laminates displayed uniform FVF, and porosity < 0.01 % (as determined by IA).

The mechanical properties of T650-35 8HS/TriA X are summarized in Table 4. Tensile and flexural strength and moduli are fiber-dominated properties, affected by stacking sequence and fiber properties. In contrast, SBS strength depends on matrix properties and fiber-matrix interfacial shear

Please cite the article as: Zhang, Y., Jain, A., Grunenfelder, L. K., Miyauchi, M., & Nutt, S.. “**Process development for phenylethynyl-terminated PMDA-type asymmetric polyimide composites,**” High Performance Polymers (2017), DOI: [10.1177/0954008317720802](https://doi.org/10.1177/0954008317720802)





strength.<sup>24</sup> In this work, mechanical testing was performed on quasi-isotropic laminates (T650-35 8HS/TriA X). Most mechanical properties for polyimide composites reported in the literature, however, are from cross-ply (0/90) laminates. To avoid differences based on fiber properties or lay-up sequence, we have focused our comparison on SBS strength, a matrix-dominated property. The room-temperature SBS strength of T650-35 8HS/TriA X (67 MPa) was 16% greater than that of T650-35 8HS/PMR-15 (58 MPa<sup>25</sup>) and 46% greater than that of T650-35 8HS/AFR-PE-4 (46 MPa<sup>26</sup>).

Table 3. Specimens for mechanical tests.

Mechanical test	ASTM standard used for testing	Lay-up sequence	Length (mm)	Width (mm)	Thickness (mm)	Number of specimens	FVF (vol%)	Void content* (%)
Tensile	D3039 <sup>18</sup>	[0/+45/-45/90] <sub>s</sub>	254.10	25.460	3.120	6	55.1	<0.01
Flexural	D7264 <sup>19</sup>	[0/90/-45/+45/0/90] <sub>s</sub>	162.30	25.058	4.607	8	55.6	<0.01
SBS	D2344 <sup>20</sup>	[0/+45/-45/90] <sub>s</sub>	17.54	5.886	3.097	5	55.1	<0.01

\* Determined by image analysis.

Table 4. Mechanical properties of T650-35 8HS/TriA X.

Property	T650-35 8HS/TriA X
Tensile strength (MPa)	515±27
Tensile modulus (GPa)	45.5±1.8
Strain-to-failure (%)	1.12±0.07
Flexural strength (MPa)	660.2±26.9
Flexural modulus (GPa)	42.0±0.9
SBS strength (MPa)	67.1±5.3

Please cite the article as: Zhang, Y., Jain, A., Grunenfelder, L. K., Miyauchi, M., & Nutt, S.. “**Process development for phenylethynyl-terminated PMDA-type asymmetric polyimide composites,**” High Performance Polymers (2017), DOI: **10.1177/0954008317720802**





## 5. Conclusions

A polymer science-based approach was employed to develop and demonstrate a process suitable for fabricating laminates with a new PMR-type polyimide resin system, TriA X. The chemorheological behavior of the TriA X system was characterized, yielding an improved understanding of resin flow in a complex reacting system and establishing connections between viscosity changes and chemical/physical reactions. This understanding guided the development of a cure cycle suitable for the fabrication of high-quality laminates. Additionally, a thermal analysis method was designed to determine the effects of B-staging temperature on resin viscosity, imidization, and crosslinking. A principle of “*maximum imidization without cross-linking*” was implemented to determine a suitable B-staging temperature. The approach we have demonstrated minimizes the material/time/energy cost of process development, while affording accurate control over resin properties in different processing conditions.

A molding cycle was designed based on the assessment of TriA X processability. The cycle was implemented, leading to complete consolidation of 8HS prepreg plies into composite laminates with  $T_g = 367\text{ }^{\circ}\text{C}$  (peak of  $\tan \delta$ ) and void content consistently  $< 0.1\%$ . The consolidated laminates exhibited room temperature matrix-dominated mechanical properties that exceeded those of conventional polyimide composites. Prior work<sup>16, 17</sup> has reported exceptional ductility (elongation-at-break of 13.5%) and tensile strength (122 MPa) of TriA X neat resin, properties that far surpass those of conventional polyimides. The exceptional mechanical properties of TriA X, and the process reported here for fabricating composite laminates using this resin system, have the potential to expand the design space, leading to new applications for polyimide composites. The system



addresses key drawbacks to prior polyimide materials as a result of the intrinsic properties of the matrix, particularly superior ductility and ability to process without carcinogenic constituents.

## 6. Acknowledgments

The authors would like to thank William Guzman of Kaneka Americas Holding, Inc., Yunpeng Zhang, and William Edwards of University of Southern California for assistance with TriA X resin preparation, mechanical testing, and micro-CT measurements, respectively. The authors acknowledge financial support from Kaneka Americas Holding, Inc.

## 7. Declaration of Conflicting Interests

The author(s) declared no potential conflicts of interest with respect to the research, authorship, and/or publication of this article.

## 8. Funding statement

The author(s) disclosed receipt of the following financial support for the research, authorship, and/or publication of this article: This work was supported by Kaneka Corporation and Henkel Corporation.

## 9. Reference

1. Abadie MJ. *High Performance Polymers-Polyimides Based-From Chemistry to Application*. InTech, 2012.
2. Serafini TT, Delvigs P and Lightsey GR. Thermally stable polyimides from solutions of monomeric reactants. *Journal of Applied Polymer Science*. 1972; 16: 905-15.
3. Wilson D. PMR-15 processing, properties and problems—a review. *British Polymer Journal*. 1988; 20: 405-16.

Please cite the article as: Zhang, Y., Jain, A., Grunenfelder, L. K., Miyauchi, M., & Nutt, S.. “**Process development for phenylethynyl-terminated PMDA-type asymmetric polyimide composites,**” *High Performance Polymers* (2017), DOI: **10.1177/0954008317720802**



4. Jang BZ, Pater RH, Soucek MD and Hinkley JA. Plastic deformation mechanisms in polyimide resins and their semi-interpenetrating networks. *Journal of Polymer Science Part B: Polymer Physics*. 1992; 30: 643-54.
5. Mills JS, Herakovitch CT and Davis Jr JG. Transverse Microcracking in Celion 6000/PMR-15 Graphite-Polyimide. DTIC Document, 1979.
6. Owens G and Schofield S. Thermal cycling and mechanical property assessment of carbon fibre fabric reinforced PMR-15 polyimide laminates. *Composites science and technology*. 1988; 33: 177-90.
7. Hsiao SH and Lin KH. Polyimides derived from novel asymmetric ether diamine. *Journal of Polymer Science Part A: Polymer Chemistry*. 2005; 43: 331-41.
8. Chern YT, Tsai JY and Wang JJ. High T<sub>g</sub> and high organosolubility of novel unsymmetric polyimides. *Journal of Polymer Science Part A: Polymer Chemistry*. 2009; 47: 2443-52.
9. Chern Y-T and Tsai J-Y. Low dielectric constant and high organosolubility of novel polyimide derived from unsymmetric 1,4-bis(4-aminophenoxy)-2,6-di-tert-butylbenzene. *Macromolecules*. 2008; 41: 9556-64.
10. Yokota R, Yamamoto S, Yano S, et al. Molecular design of heat resistant polyimides having excellent processability and high glass transition temperature. *High Performance Polymers*. 2001; 13: S61-S72.
11. Ogasawara T, Ishikawa T, Yokota R, et al. Processing and properties of carbon fiber reinforced triple-A polyimide (Tri-A PI) matrix composites. *Advanced Composite Materials*. 2002; 11: 277-86.



12. Chuang KC, Criss Jr JM and Mintz EA. Polyimide composites based on asymmetric dianhydrides (a-ODPA vs a-BPDA). *Society for the Advancement of Material and Process Engineering Conference Proceedings*. Baltimore, MD 2009.
13. Miyauchi M, Kazama K-i, Sawaguchi T and Yokota R. Dynamic tensile properties of a novel KAPTON-type asymmetric polyimide derived from 2-phenyl-4,4'-diaminodiphenyl ether. *Polymer journal*. 2011; 43: 866-8.
14. Miyauchi M, Ishida Y, Ogasawara T and Yokota R. Novel phenylethynyl-terminated PMDA-type polyimides based on KAPTON backbone structures derived from 2-phenyl-4,4'-diaminodiphenyl ether. *Polymer journal*. 2012; 44: 959-65.
15. Miyauchi M, Ishida Y, Ogasawara T and Yokota R. Highly soluble phenylethynyl-terminated imide oligomers based on KAPTON-type backbone structures for carbon fiber-reinforced composites with high heat resistance. *Polymer journal*. 2013; 45: 594-600.
16. "Structure and properties of phenylethynyl-terminated PMDA-type asymmetric polyimide", Zhang Y and Nutt SR, unpublished work.
17. Zhang Y, Jain A, Guzman W, et al. Processing and properties of phenylethynyl-terminated PMDA type polyimide composites. *Society for the Advancement of Material and Process Engineering Conference Proceedings*. Long Beach, CA 2016.
18. Houlihan F, Bachman B, Wilkins Jr C and Pryde CA. Synthesis and characterization of the tert-butyl ester of the oxydianiline/pyromellitic dianhydride polyamic acid. *Macromolecules*. 1989; 22: 4477-83.



19. Omote T, Yamaoka T and Koseki K. Preparation and properties of soluble and colorless fluorine-containing photoreactive polyimide precursors. *Journal of applied polymer science*. 1989; 38: 389-402.
20. ASTM. D3039 Standard test method for tensile properties of polymer matrix composite materials. American Society for Testing and Materials.
21. ASTM. D7264 Standard test method for flexural proper-ties of polymer composite materials. American Society for Testing and Materials.
22. ASTM. D2344 Standard test method for short-beam strength of polymer matrix composite materials and their laminates. American Society for Testing and Materials.
23. Hou T, Wilkinson S, Johnston N, Pater R and Schneiderk T. Processing and properties of IM7/LARC™-RP46 polyimide composites. *High Performance Polymers*. 1996; 8: 491-505.
24. Ahmed KS and Vijayarangan S. Tensile, flexural and interlaminar shear properties of woven jute and jute-glass fabric reinforced polyester composites. *Journal of materials processing technology*. 2008; 207: 330-5.
25. CYCOM® 2237 Polyimide Resin System Technical Data Sheet. *Cytec Solvay Group*. 2012: 1-7.
26. AFRPE®-4 Prepreg Data Sheet. *PROOF Research's Advanced Composite Division (formerly P<sup>2</sup>SI)*. 1-3.